



Simultaneous degradation of toxic organic pollutants by thin-falling-water-film DBD reactor

Antonio Mercado-Cabrera^a, Bethsabet Jaramillo-Sierra^b, Rosendo Peña-Eguiluz^{a,*}, Régulo López-Callejas^a, Benjamín Gonzalo Rodríguez-Méndez^a, Raúl Valencia-Alvarado^a, Alma Neli Hernández-Arias^b, Arturo Eduardo Muñoz-Castro^a

^aInstituto Nacional de Investigaciones Nucleares, Plasma Physics Laboratory AP 18-1027, 11801 CDMX, Mexico, emails: rosendo.eguiluz@inin.gob.mx (R. Peña-Eguiluz), antonio.mercado@inin.gob.mx (A. Mercado-Cabrera), regulo.lopez@inin.gob.mx (R. López-Callejas), benjamin.rodriguez@inin.gob.mx (B.G. Rodríguez-Méndez), raul.valencia@inin.gob.mx (R. Valencia-Alvarado), arturo.munoz@inin.gob.mx (A.E. Muñoz-Castro)

^bTecnológico de Estudios Superiores de Tianguistenco, Carretera Tenango-La Marquesa km 22, 52650, Santiago Tianguistenco, Estado de México, Mexico, emails: beth_jasi@yahoo.com.mx (B. Jaramillo-Sierra), nelly.alama@hotmail.com (A.N. Hernández-Arias)

Received 9 August 2017; Accepted 6 December 2017

ABSTRACT

The theoretical and experimental studies of the simultaneous degradation of phenol and *m*-cresol in an aqueous solution only using a non-thermal plasma of dielectric barrier discharge (DBD) in a gas-liquid interaction are presented. A thin-falling-water-film reactor in tube-cylinder configuration was used; the mixture of phenol and *m*-cresol in an aqueous solution was driven to a DBD reactor by a submersible pump from a reservoir. The non-thermal plasma was generated in Ar/O₂ gas mixtures on the liquid surface. The intermediates were analyzed by solid-phase extraction and gas chromatography-mass spectrometry. The highest degradation efficiency of 99% for both components was obtained by supplying only O₂. It was observed that phenol degradation preceded the *m*-cresol oxidation during the first minutes of the process. The results are discussed with the logarithmic acid dissociation constant pK_a and the structure of the compound. A proposed chemical kinetics model allows us to verify that the removal of contaminants began with phenol followed by *m*-cresol.

Keywords: Simultaneous degradation; Organic pollutants; DBD reactor; Plasma

1. Introduction

Phenol and *m*-cresol are organic compounds widely used in chemical, petrochemical, pharmaceutical and cosmetic industry [1,2] and the residual derived from their exploitation may be present in wastewater. They are considered as priority pollutants in some countries such as United States [3], Canada, and the European Union [4] because of its high toxicity and low biodegradability [5–7], affecting the health of living beings. It is known that chlorination process can generate even more toxic and difficult compounds to remove

by its reaction with residual chemical compounds during the tertiary treatment of wastewater [8,9]. Therefore, as an effort to promote a healthy environment, it is crucial to implement efficient alternative technologies friendly to the environment.

The non-thermal plasma, also called cold plasma, is a collection of electrons, ionized and excited species, and free radicals that can react with contaminants contained in air, in water and even in the soil to form less toxic species. The non-thermal plasma can be generated mainly by electric discharges such as dielectric barrier discharge (DBD) and pulsed corona discharge. The reactor configuration influences several physical characteristics of the electric discharge which in turn promotes the generation of chemical species in the function of the supplied gases mixture.

* Corresponding author.

These properties have a great influence on the effectiveness of the plasma process.

The non-thermal plasma for wastewater treatment may be generated (a) on the water surface, (b) inside the water when both electrodes are immersed in the liquid and (c) bubbling reactive gas in the liquid [10]. Gas mixtures containing oxygen are mainly used with the aim of generating $\cdot\text{OH}$ radicals. The $\cdot\text{OH}$ radical is considered as the main oxidation chemical species of contaminants because it is lesser selective concerning other active species such as ozone (O_3).

In the case of pollutants in water, the oxidation mechanism is promoted by various phenomena generated by the electric discharge, such as UV radiation, high local temperature, intense shock wave propagating in the liquid (as in the submerged electrodes device) and all cases mainly due to chemical interactions with oxidizing molecular species (H_2O_2 and O_3) and free radicals ($\cdot\text{OH}$, $\cdot\text{O}$ and $\cdot\text{H}$) [11,12]. These species have higher oxidation potentials than that of commonly used chemicals in the wastewater treatment and can be generated in advanced oxidation processes (AOP) [13]. It is necessary in several cases that the combined action with chemical reagents to increase the removal efficiency of AOP (e.g., H_2O_2 , Fe^{2+} , TiO_2 , etc.), sometimes including additional stages of cleaning or filtration of the effluent [14,15], in addition to the mandatory use of another source of energy, usually in the form of UV radiation.

Non-thermal plasma can be considered in the category of AOP, with the advantage that the process is carried out in a single stage and the generation of UV radiation, active species and free radicals previously mentioned are generated in situ and practically without the need of any complementary stage. Several works have been developed to validate the effectiveness of non-thermal plasma which has focused mainly on: organic compounds [16], herbicides [17,18], pesticides [19], dyes [10,20,21], pharmaceuticals and personal care products [22]. Furthermore, there are some other works in the literature describing the treatment of synthetic aqueous solutions by non-thermal plasma for the removal of multiple organic pollutants, but all of them individually treated [23–26]. Until now, few number of studies have been reported on the simultaneous degradation of contaminants in water, one of them is based on direct ozonolysis [27] using an ozone contactor, other on biodegradation [28] and another on a photocatalytic process [29]. Wastewater coming from chemical industry may be formed by a complex mixture of organic contaminants, and any treatment becomes a challenge due to the different chemical interactions that can take place between a mixture of contaminants and by-products. It is essential to pay attention to selectivity, reactivity and chemical structure of the compounds to be decomposed by the implemented degradation process for two or more pollutant compounds.

In this work, a simultaneous degradation of a mixture of phenol and *m*-cresol in aqueous solution using a thin-falling-water-film DBD reactor to generate non-thermal plasma on the surface of the aqueous solution was carried out. The simultaneous phenol and *m*-cresol degradation due to the Ar/O_2 gases mixture effect, treatment time and electric power consumed was assessed. Previously, the degradation of phenol and *m*-cresol in aqueous solutions was analyzed separately [30,31]. The intermediates of reaction were analyzed by solid-phase extraction (SPE) and gas chromatography–mass spectrometry.

The results were discussed relating the acidity of each compound and the reactivity of the functional groups present in the aromatic ring. A simplified kinetic model for the liquid phase using only reaction rate constants and species concentration to explain the obtained experimental results is proposed.

2. Methods and materials

2.1. Experimental device

The experimental device used in this work is shown in Fig. 1. It is constituted by (a) a gas supply system for the treatment reactor; (b) a power supply system able to generate an AC amplitude voltage up to 25 kV at 1.5 kHz of frequency; where the electrical characteristics were measured using a TDS2014 digital oscilloscope coupled to a high-voltage probe P6015A 1,000:1, both from Tektronics, Inc. (OR USA) and, a 1.0 V A⁻¹ current transformer from Pearson Electronics, Inc. (Palo Alto, CA, USA); (c) a thin-falling-water-film reactor of cylindrical structure consisting of a \varnothing_{ext} 12.00 mm hollow stainless steel tube working as the high-voltage polarized electrode; a grounded electrode made of a fine copper mesh covering a \varnothing_{ext} 22.0 mm quartz tube used as a dielectric material and, a 3.5 mm gas gap; and (d) a gas chromatograph GC 6890N coupled to mass detector MSD 5973N (GC/MS), with an HP-5MS capillary column with the purpose to analyze the collected liquid samples.

2.2. Methodology

A 500 mL of aqueous solution containing a mixture of the two abovementioned organic compounds was prepared from purified water, being the initial concentrations of phenol and *m*-cresol, respectively, of $\sim 5 \times 10^{-3}$ mol L⁻¹ and 1×10^{-3} mol L⁻¹. All chemicals used in this experiment were of analytical grade (phenol Fermont 99.0%, *m*-cresol J.T. Baker 99.9%, methanol J.T. Baker 99.93%, acetone J.T. Baker 99.93%). Conductivity and pH of all aqueous solutions were measured before non-thermal plasma treatment using a pH/conductivity meter Horiba D-54, the obtained average magnitudes were, respectively, ~ 0.0264 S m⁻¹ and ~ 7.2 . H_2O_2 concentration after treatment was measured with Insta-TEST hydrogen peroxide test strips. Each aqueous solution was treated for 1 h in the thin-falling-water-film reactor wherein a DBD non-thermal plasma was generated in Ar/O_2 gas mixture, and water film becomes the second dielectric. The aqueous solution was pumped inside the hollow high-voltage electrode until reaching its top and falling through the outer wall of the electrode forming a thin film of aqueous solution. In this work, the degradation of a mixture of organic compounds in aqueous solution was analyzed, considering the effect of four different gas mixture compositions of Ar/O_2 that were: (a) 100% Ar–0% O_2 , (b) 90% Ar–10% O_2 , (c) 80% Ar–20% O_2 and (d) 0% Ar–100% O_2 . In all cases, the supplied gas mixture flow to the plasma reactor was kept constant at 1 L min⁻¹. For a selected gas mixture three experiments were done, each at a constant power during 1 h of treatment. The supplied electric power was controlled by adjusting the voltage magnitude applied at a constant frequency of 1.5 kHz. Liquid samples were collected for every 5 min until a half-hour and then every 10 min until an hour of treatment time and analyzed by GC/MS during the non-thermal plasma treatment.

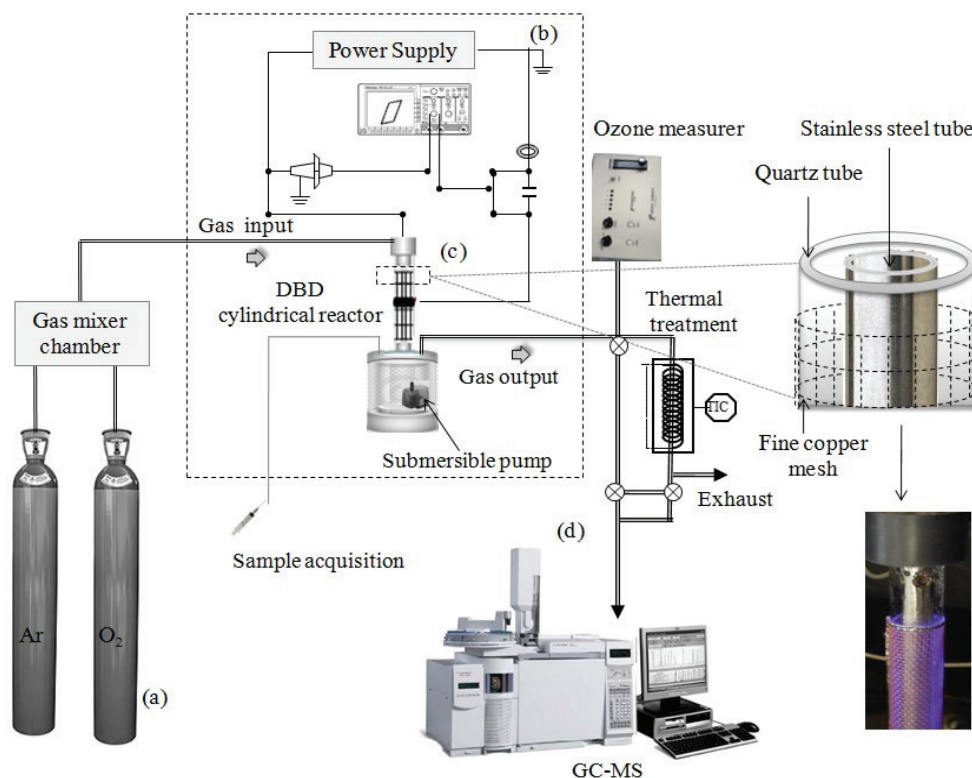


Fig. 1. Experimental device.

It must be noted that degradation efficiency in percentage (%) of each organic compound was obtained from:

$$\eta = \frac{A_0 - A_t}{A_0} \times 100\% \quad (1)$$

where η indicates the obtained efficiency in (%), A_0 is the initial abundance of the contaminant and A_t is the abundance of the contaminant obtained at time t during and after non-thermal plasma treatment.

By-products identification was accomplished with tC18 cartridge SPE for GC–MS system. Hence, every treated aqueous solution was passed through a previous conditioned cartridge with 6 mL of methanol ACS, a following two-step elution phase was implemented beginning with 3 mL of methanol and ending with 3 mL of acetone both ACS grade. Then, the analysis was performed injecting a sample of 1 μ L of the obtained extract in the GC–MS system.

2.3. Theoretical model

The kinetic model is based on the equation of species conservation, in this work, it was only considered for the liquid phase; this equation describes the concentration change of a chemical species “ i ” at the time t :

$$\frac{dC_i}{dt} = S_i \quad (2)$$

where C_i is the molar density of species “ i ” and, S_i represents the molar balance for species “ i ” which is only function of

the species molar concentrations and the reaction rate coefficients k . These coefficients were consulted from the literature [32–39]. The proposed model consisted of 67 chemical species and 44 chemical reactions evolving in the liquid phase. Rosenbrock’s method [40,41] was used for stiff ordinary differential equations solver. It is important to note that Eq. (2) is a zero-dimensional model and only represents a balance of species in a time t , where the volume of the solution is constant. Although this is a very simplified model, it allows us, on the one hand, to have a knowledge of the interaction of the parallel reactions, and, on the other hand, to anticipate the reaction pathway of the target compounds as well as to the intermediaries that are generated doing use of reaction rate coefficients consulted from the literature.

3. Results and discussion

3.1. Experimental results

When an organic mixture of phenol and *m*-cresol is simultaneously treated in the same aqueous solution by DBD non-thermal plasma, normally a higher degradation efficiency was obtained when greater the electric power and the treatment time, as it is depicted in Fig. 2. For a gas mixture composed only of argon (100% Ar–0% O₂), the oxidation process of the mixture of contaminants in aqueous solution was carried out, although separately incorporated in aqueous solution the compounds were oxidized as an organic mixture. The removal efficiencies in the mixture for each compound were up to 82% of phenol and 84% for *m*-cresol. Moreover, in another series of experiments it was increased the percentage

of oxygen, as a result, it can be observed from Fig. 3 that a small amount of O₂ allowed increasing the oxidation appreciably for each compound. In a first instance for 90% Ar–10% O₂ gas mixture the additional electric power is consumed for the dissociation and generation of other species from O₂, which results in an apparent decrease of elimination efficiency (%). Also, the utilized power also generates heat that can cause vaporization of the aqueous solution making the plasma unstable in comparison with an argon plasma. That is why a mixture under these conditions (Ar/O₂) requires more electric power to sustain a stable discharge, which exceeding 20 W begins to denote the beneficial effect of O₂. Thus for the case of a gas mixture of 90% Ar–10% O₂ and with a supplied electric power of 23.3 W, the maximum attained degradation efficiencies, respectively, for phenol and *m*-cresol were 86.5% and 94.6%. As previously mentioned, a variety of oxidant species such as [•]O, [•]OH, O₃ and H₂O₂ are generated by the plasma–liquid interaction and transferred to the aqueous phase by diffusion.

Taking into account the obtained results from 100% Ar–0% O₂ and 90% Ar–10% O₂, it can be noticed that for 100% Ar–0% O₂, the argon allowed the generation of free radicals and reactive species necessary for oxidation, presumably [•]OH radical and H₂O₂, as it will be seen later (section 3.3), mainly due to the formation of quinones in the residual solution. Also, for 100% Ar–0% O₂, a generation of H₂O₂ up to 30 ppm was detected, as well as the increase in conductivity of 0.0264 to 0.0463 S m⁻¹ and a decrease in pH, whereas ozone (O₃) was not detected in outlet gas. For gas mixture 90% Ar–10% O₂ ozone (O₃) was formed and detected in the gas phase, and it can be diffused in the liquid phase to generate [•]OH radical, the water molecules of the gas–liquid interface also generate radicals [•]OH:

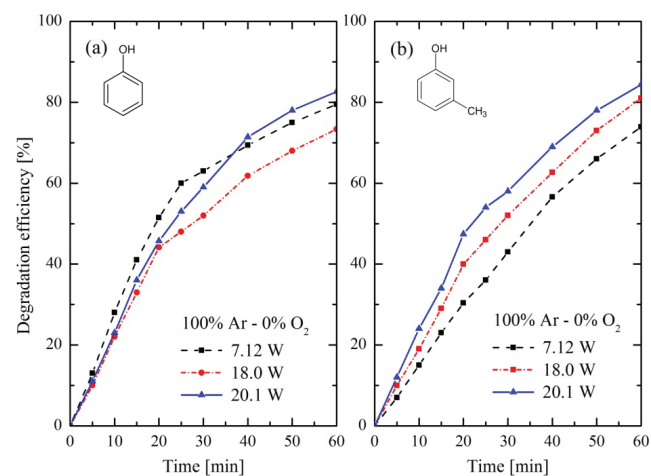


Fig. 2. Simultaneous degradation of (a) phenol and (b) *m*-cresol by non-thermal plasma at 100% Ar–0% O₂ in the function of treatment time and applied electric power.

Moreover, water molecules in the liquid phase move to the gas–liquid interface, where some of them are transferred to the gas phase by evaporation, later dissociated by electron impact:



The oxidation process of the mixture of pollutants is thought to be carried out via the electrophilic addition of [•]OH radicals to the aromatic ring. Some authors have observed that when the gas mixture consists mostly of Ar, the responsible species for the oxidation are [•]OH radicals which have a high oxidizing potential and their reaction are non-selective on organic compounds [42,43].

In Fig. 4, the results of the degradation efficiency of phenol and *m*-cresol in the gas mixture 80% Ar–20% O₂ are shown. It can be observed that the degradation efficiencies rose up to 93.0% for phenol and 99.0% for *m*-cresol. These last

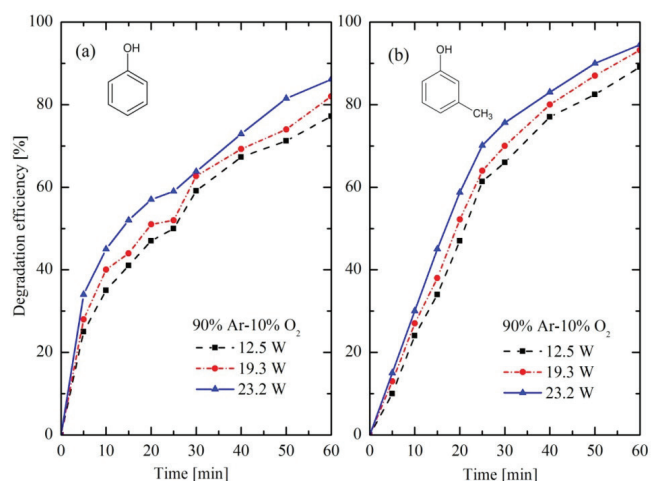


Fig. 3. Simultaneous degradation of (a) phenol and (b) *m*-cresol by non-thermal plasma at 90% Ar–10% O₂ in the function of treatment time and applied electric power.

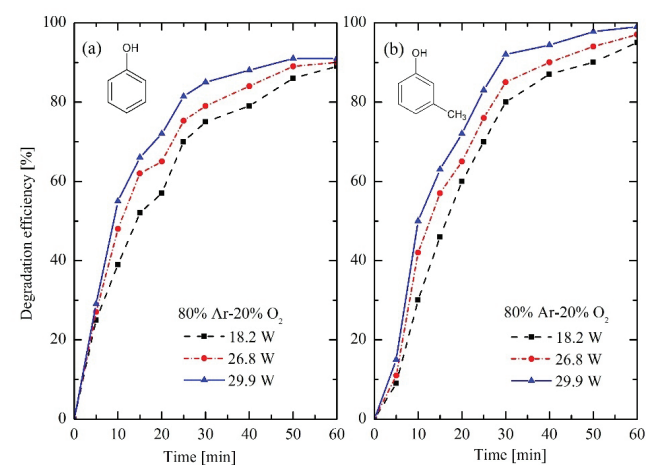


Fig. 4. Simultaneous degradation of (a) phenol and (b) *m*-cresol by non-thermal plasma at 80% Ar–20% O₂ in the function of treatment time and applied electric power.

values were higher than those previously obtained with the others gas mixtures.

It should be pointed out that the initial concentration of *m*-cresol was five times lower than that of phenol. This difference may contribute to the fact that after 1 h of treatment time the *m*-cresol degradation was higher than phenol degradation, as it can be noticed comparing results from Figs. 2–4. Moreover, it is observed in the same figures, that phenol was degraded slightly faster during the first minutes of treatment despite having a five times higher concentration than *m*-cresol. Finally, after 1 h of treatment time, high levels of phenol degradation comparable with those for *m*-cresol were reached. Based on correlation reactivity-acid dissociation constant pK_a and reactivity-chemical structure, the results can be explained as follows:

- The reactivity of phenol and *m*-cresol can be estimated by the acid dissociation constant pK_a . It has been observed that compounds with low pK_a values are easily degraded by oxidation. In this case, some pK_a values are given in Table 1 [44], others substituted phenols in Table 1 are taken only as reference, wherein, the pK_a value of phenol is slightly lower than that for *m*-cresol ($pK_{a(\text{phenol})} < pK_{a(m\text{-cresol})}$). For the case studied in this work, this would mean that phenol oxidation occurs before oxidation of *m*-cresol, hence, the firsts generated by-products correspond to those of phenol oxidation, which mainly are: catechol, resorcinol and hydroquinone. Also, observing their pK_a values, these last compounds are more susceptible to be degraded by oxidation than *m*-cresol. The effect of the acid dissociation can be increased by the decrease of the pH in the aqueous solution at the end of the experimental procedure, besides the difference of concentration of phenol and *m*-cresol used in this work. Other studies have shown that it is necessary to take into account that the other factors such as chemical structure and the constant of reaction are important to clearly state the reactivity of

a substituted phenol especially the nature of substituent, that is, nitrophenols are less reactive than phenol despite the difference in their pK_a [26,27].

- The chemical reactivity of the organic compound due to the position of the substituent on the aromatic ring. For substituted phenols these values are quantified by the inductive and resonance effects given by the Hammett constants (σ), the σ_m and σ_p values are indicative of the substituent behaves as an electron-donor or electron-acceptor substituent. Values σ_m and σ_p for non-substituted phenol are considered as zero [26,45] (Table 2).

Due to the difference in electronegativities of oxygen (in -OH substituent) and carbon (in -CH₃ substituent) on the aromatic ring, the stronger inductive effect is of the substituent -OH. From Table 2, it can be noted that the absolute values of σ_m and σ_p corresponding to the -OH group are greater than those of the -CH₃ group. Particularly, the group -OH is a weak deactivator in *meta*-position and electron-donor in *para*-position, this last increases the electron density in the aromatic ring and therefore its reactivity, contrary to the -CH₃ group which is a weak activator in *meta*-position. From other studies [46], it is known that *ortho*- and *para*-positions are more reactive to oxidation attack, the first one, due to the increase of the field effect and the second one, due to the resonance effect. In the *meta*-position the effects are balanced, and *m*-cresol is less active than catechol and hydroquinone.

In the particular case of study in this work, it seems to favor in a first instance the effect of pK_a . After 15 min of non-thermal plasma treatment, the pollutants concentrations have a certain influence over the global oxidation process. Thus, as a result, the obtained final degradation efficiency for *m*-cresol is higher in all cases than phenol removal, as it can be seen in Figs. 2–4.

Fig. 5 shows the results when the gas mixture was only constituted by O₂ (that was 0% Ar–100% O₂), where efficiencies of up to 99.2% for phenol and 99.6% for *m*-cresol were obtained. From the characteristic curve of these results, it can be observed a similar removal behavior respect to preceding experiments, the increase of the treatment time and supplied electric power has a favorable effect on the efficiency of degradation. It is also observed that in the first 10 min of treatment, phenol degradation was higher than *m*-cresol removal. Some authors have observed that catechol and hydroquinone (secondary by-products of phenol oxidation) are highly reactive with ozone by several orders of magnitude compared with other chemical compounds ($3.1 \times 10^3 \text{ M}^{-1} \text{ s}^{-1}$ for catechol and $1.5 \times 10^6 \text{ M}^{-1} \text{ s}^{-1}$ for hydroquinone) [47], once these

Table 1
Acid dissociation constant (pK_a) of several compounds

Substituted phenol	pK_a
Catechol	9.34
Resorcinol	9.32
Hydroquinone	9.85
Phenol	9.99
<i>o</i> -cresol	10.29
<i>m</i> -cresol	10.09
<i>p</i> -cresol	10.26
2-Chlorophenol	8.56
3-Chlorophenol	9.12
4-Chlorophenol	9.41
2-Nitrophenol	7.23
3-Nitrophenol	8.36
4-Nitrophenol	7.15
2-Aminophenol	4.78
3-Aminophenol	4.37
4-Aminophenol	5.48

Table 2
Hammett constants values for phenol and substituted phenol

Substituent	σ_m	σ_p
Phenol	0	0
-CH ₃	-0.07	-0.17
-OH	0.12	-0.37
-Cl	0.37	0.23
-NO ₂	0.71	0.78
-NH ₂	-0.16	-0.66

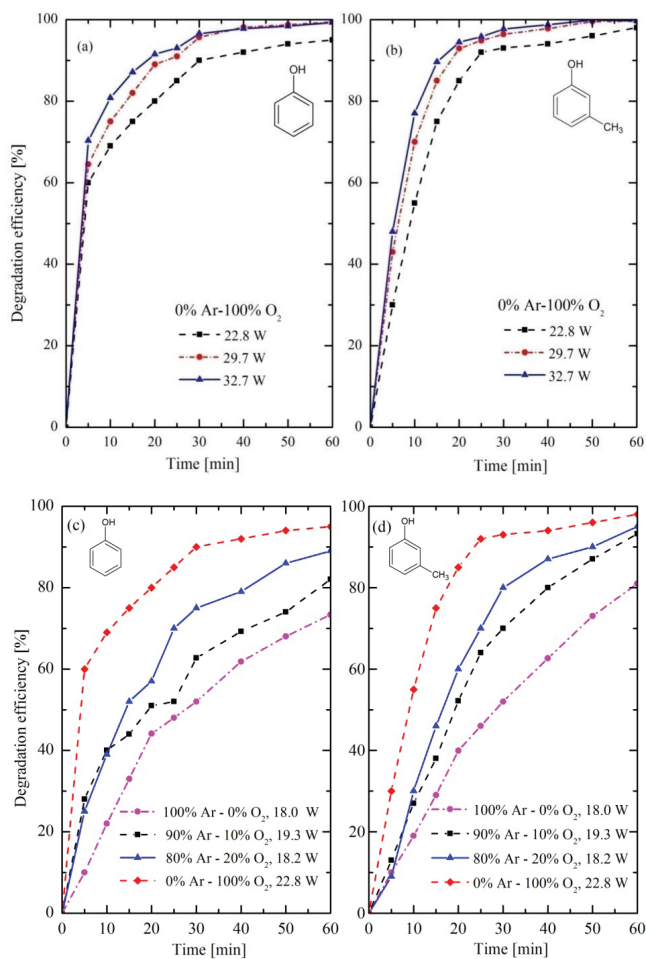


Fig. 5. Simultaneous degradation of (a) phenol and (b) *m*-cresol by non-thermal plasma at 0% Ar–100% O₂ in the function of treatment time and applied electric power. (c) and (d) Effect of O₂ in the gas mixture Ar/O₂ on degradation efficiency for phenol and *m*-cresol.

compounds are generated in the solution affect the oxidation of *m*-cresol. For the particular case of 0% Ar–100% O₂, pH up to 3.0 and conductivities up to ~0.112 S m⁻¹ were measured. In Figs. 5(c) and (d), the effect of increasing the O₂ ratio is observed, in the figure shown for both phenol (c) and *m*-cresol (d), the tendency in gas mixture efficiency is as follows: O₂ > Ar/O₂ > Ar. Considering that in Ar/O₂ mixture, when the proportion of O₂ increased, the efficiency of degradation of the considered organic mixture also increased.

Unlike a typical ozonation process, the emission of UV radiation from non-thermal also allows to accelerate the decomposition of O₃ to generate [48]:



The species $\cdot\text{O}({}^1\text{D})$ is highly reactive and has a high impact on the chemistry of the process in the presence of H₂O:



The above process can provide free radicals ($\cdot\text{OH}$) even at low pH, contributing to the overall oxidation process.

When the composition of the gas mixture was only constituted by oxygen, the degradation is mainly attributed to ozone, which is generated in abundance during the electric discharge in the gas phase (Fig. 6) and, then diffused in the liquid phase. Ozone has two oxidation pathways: on the one hand directly with the pollutant and, on the other hand indirectly through its decomposition into the water forming $\cdot\text{OH}$ radicals [42,49]. Ozone, being a particular species attacks organic compounds with high electronic densities and activated aromatic systems such as phenol. The degradation mechanism of organic compounds by a direct attack by ozone is based on the rupture of the aromatic ring.

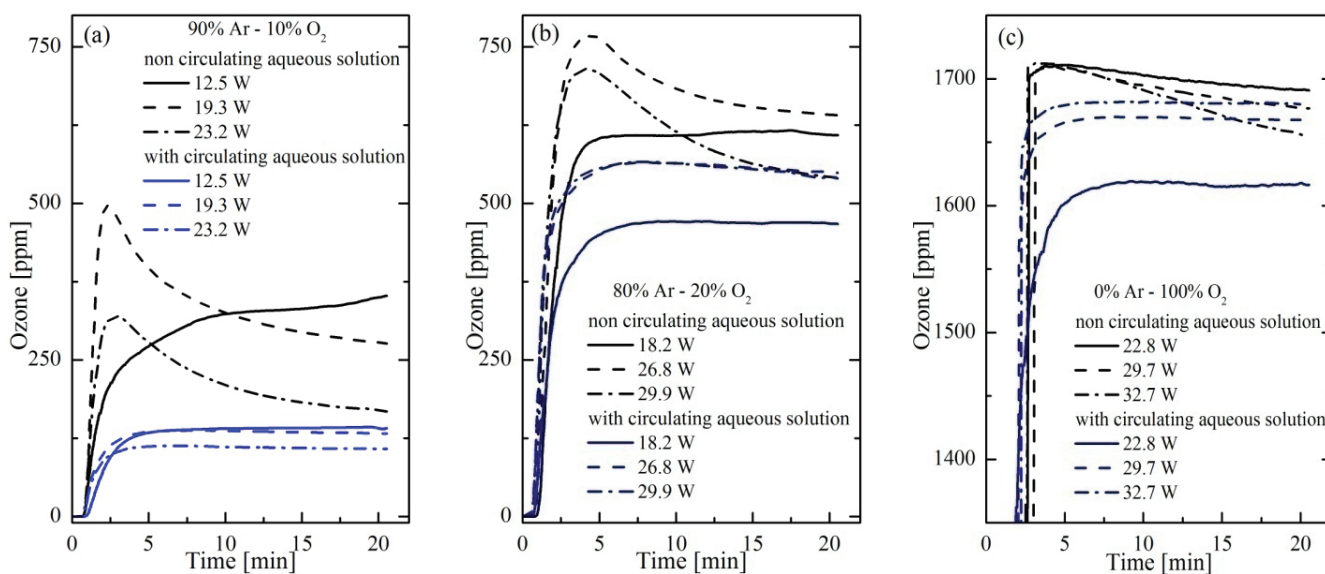


Fig. 6. Ozone generation in the function of gas mixture and applied electric power for: (a) 90% Ar–10% O₂, (b) 80% Ar–20% O₂ and (c) 100% O₂.

As mentioned above, the oxygen present in the gas phase promotes the generation of active species such as $\cdot\text{O}$ and O_3 , which are directly related to the formation of radicals $\cdot\text{OH}$, therefore, to the degradation of pollutants. Fig. 6 shows the generation of ozone as a function of the gas mixture and the applied electric power, for two different cases, when there was only a gas phase and when there was an aqueous solution circulating on the surface of the electrode. From the outcomes, it was observed the higher the oxygen concentration, the higher the ozone generation. The decrease of O_3 at the gas output when there is flowing aqueous solution in comparison when there is not an aqueous solution is shown in Figs. 6(a)–(c). This dissimilarity can be explained as follows: (a) the diffused O_3 into the water promotes the generation of reactive species (H_2O_2) and free radicals ($\cdot\text{OH}$) and (b) O_3 was consumed from direct oxidation process and cleavage of the aromatic ring. It was also observed that when Ar relation was increased in the gas mixture, the production of O_3 decreased. This could be mainly due to the energy distribution between Ar and O_2 , which causes that some O_2 excitation–dissociation processes are not carried out at the same efficiency as when only O_2 is present in the gas mixture. When the gas mixture was composed only of Ar gas, O_3 was not detected.

Fig. 7 summarized degradation efficiency obtained by the simultaneous oxidation of phenol and *m*-cresol at 20, 40 and 60 min of non-thermal plasma treatment. For each gas mixture and in all cases, it was tried to apply an electric power magnitude within a difference range about 1 W, except for the case of 100% O_2 where the minimal consumed power to generate plasma was 22.8 W. Even though, this case was also compared with the other three cases, maintaining in mind that the different consumed power values were slightly lower but very close to each other.

To validate the use of the applied energy, the factor G , commonly used to evaluate the removal efficiency concerning energy, was estimated, which is a good parameter to evaluate the results of this work. The factor G (mol J^{-1}), defined in Hoeben et al. [50], is the amount of matter removed per unit of supplied input energy and is represented by:

$$G = \frac{x \cdot C_0 \cdot \text{Vol}}{E \cdot f \cdot tm} \quad (10)$$

Table 3
G factor evaluation of removal efficiency for phenol

Technique	Pulsed corona in air on water	Pulsed corona in argon on water	Pulsed corona in oxygen on water	Hybrid gas/liquid discharge	AC discharge in gas on water	DBD in gas Ar/O ₂ (100-0) on water	DBD in gas Ar/O ₂ (90-10) on water	DBD in gas Ar/O ₂ (80-20) on water	DBD in gas Ar/O ₂ (0-100) on water
C_0 (mol L^{-1})	1.0E-3	1.0E-3	1.0E-3	1.0E-3	5E-4	5.0E-3	5.0E-3	5.0E-3	5.0E-3
Vol (L)	0.100	0.100	0.454	0.550	0.070	0.500	0.500	0.500	0.500
E (J)	5.8E-3	0.0106	1.07	1.06	0.038	0.012	0.012	0.012	0.015
f (Hz)	100	100	60	60	50	1,500	1,500	1,500	1,500
t_{50} (min)	82	45	9	14	41	24	19	14	4
G_{50} (mol J^{-1})	1.75E-8	1.72E-8	6.55E-9	5.15E-9	3.7E-9	4.8E-8	5.68E-8	8.1E-8	2.2E-7
Reference	[50]	[50]	[51]	[52]	[53]	This work	This work	This work	This work

where x is considered equal to 0.5 for a 50% removal, tm is the time required for a 50% removal in s, C_0 is the initial concentration in mol L^{-1} , Vol is the volume of the aqueous solution in L, E is the supplied input energy in J and f is the frequency of the supplied voltage waveform in Hz.

Table 3 shows the results of some other techniques compared with the one proposed in this work on the elimination efficiency for phenol; likewise, Table 4 shows the results on the obtained elimination efficiencies for *m*-cresol.

3.2. Theoretical degradation

Fig. 8 shows the obtained results using Eq. (2), for the initial concentrations: $5 \times 10^{-3} \text{ mol L}^{-1}$ phenol and $1 \times 10^{-3} \text{ mol L}^{-1}$ *m*-cresol, where the theoretical degradation and the intermediates generated during the oxidation of both pollutants are observed. There are shown just as phenolic species. It is important to note that the theoretical model was performed only in liquid phase.

The mechanism begins in the gas phase where the first free radicals ($\cdot\text{O}$, $\cdot\text{OH}$ and $\cdot\text{H}$) and reactive species such as O_3 are formed by the effect of the non-thermal plasma in the gas mixture Ar/O₂ and in the H_2O diffused in the gas phase.

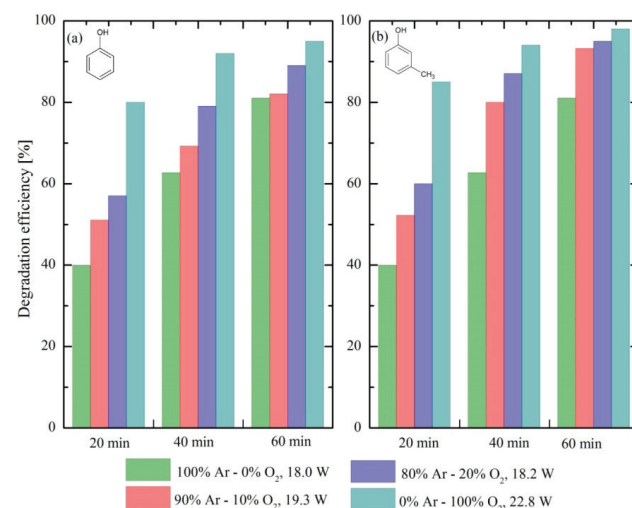


Fig. 7. Comparison of the efficiency obtained from the simultaneous oxidation of (a) phenol and (b) *m*-cresol.

Table 4
G factor evaluation of removal efficiency for *m*-cresol in this work

Technique	DBD in gas Ar/O ₂ (100-0)	DBD in gas Ar/O ₂ (90-10)	DBD in gas Ar/O ₂ (80-20)	DBD in gas Ar/O ₂ (0-100)
C ₀ (mol L ⁻¹)	1.0E-3	1.0E-3	1.0E-3	1.0E-3
Vol (L)	0.500	0.500	0.500	0.500
E (J)	0.012	0.012	0.012	0.015
f (Hz)	1,500	1,500	1,500	1,500
t ₅₀ (min)	29	19	16	9
G ₅₀ (mol/J)	7.9E-9	1.2E-8	1.4E-8	2.0E-8

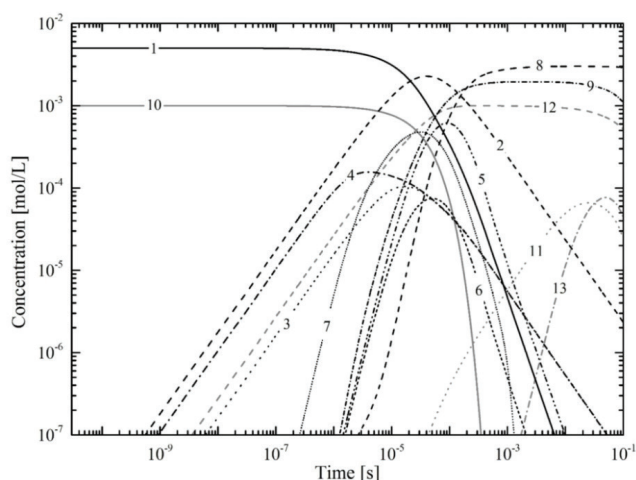


Fig. 8. Main formed species: (1) phenol (5×10^{-3} mol L⁻¹), (2) *o*-C₆H₅(OH)₂, (3) *m*-C₆H₅(OH)₂, (4) *p*-C₆H₅(OH)₂, (5) catechol, (6) resorcinol, (7) hydroquinone, (8) *p*-benzoquinone, (9) *o*-benzoquinone, (10) *m*-cresol (1×10^{-3} mol L⁻¹), (11) (3Z)-3-methyl-2,5-dioxohex-3-enedioic acid, (12) 2-methylbenzene-1,4-diol and (13) 2-methylcyclohexa-2,5-diene-1,4-dione.

These chemical species are dissolved in the liquid phase by mass transfer processes, where they can generate other reactive species such as H₂O₂ and other free radicals such as [•]OH and HO₂[•]. In addition to a direct effect of O₃ on the organic pollutants under consideration and the effect of UV emission generated by the plasma.



The free radicals formed in the aqueous solution and the reactive species will react with the organic compounds [47,54,55]:



Taking into consideration Fig. 8, it is seen that phenol (1) began to oxidize before ($t \sim 10^{-6}$ s) that *m*-cresol (10), thereby the first by-products generated were from phenol oxidation (6), (7) and (8). They presented generation rates slightly higher in relation to *m*-cresol ($1.4 \times 10^{10} \text{ M}^{-1} \text{ s}^{-1}$), mainly due to the reactivity of phenol with [•]OH radicals ($1.8 \times 10^{10} \text{ M}^{-1} \text{ s}^{-1}$). These generated intermediates (6), (7) and (8) are also highly reactive toward [•]OH radicals (1.1×10^{10} , 1.2×10^{10} , $9.80 \times 10^9 \text{ M}^{-1} \text{ s}^{-1}$, respectively) [54]. It is observed in Fig. 8 that 2-methylbenzene-1,4-diol (12) was the first generated by-product from *m*-cresol. Finally, *m*-cresol was completely oxidized after a time $t \sim 3.5 \times 10^{-4}$ s while phenol needed a larger period of time $t \sim 7 \times 10^{-3}$ s. In Fig. 8, *m*-cresol has a higher degradation with regard to phenol, even when this had been the first compound to begin oxidation process. These theoretical results are in agreement largely with that observed experimentally from the perspective of the behavior of degradation, as shown in Figs. 2–5, phenol begin to oxidize faster than *m*-cresol. Nevertheless, this last had higher elimination efficiency.

3.3. Studies of species generated from oxidation

Fig. 9 shows the chromatograms obtained by GC-MS of phenol and *m*-cresol oxidation in a mixture considering the four different gas mixture compositions studied in this work. The results are presented separated in two different retention time segments, where (a) and (b) correspond to the analysis just after treatment while (c) and (d) were obtained from the analysis performed a few hours later. Figs. 9(a) and (b) show the generation of intermediate by-products such as catechol and hydroquinone, produced by the hydroxylation of phenol and 2-methylbenzene-1,4-diol, 3-methylbenzene-1,2-diol, 4-methylbenzene-1,2-diol and 5-methylbenzene-1,3-diol by the oxidation of *m*-cresol. All these mentioned species can

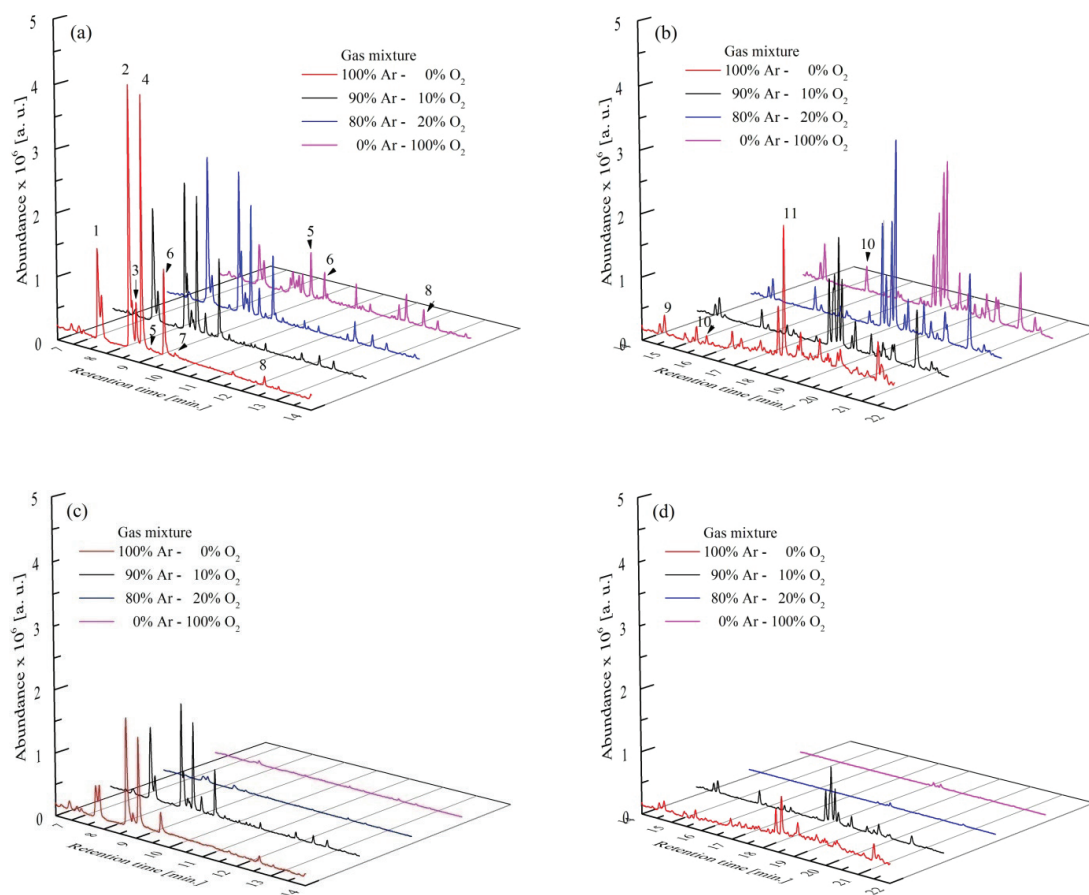


Fig. 9. GC/MS chromatograms by-products of phenol and *m*-cresol organic mixture oxidation (a) and (b) after treatment; (c) and (d) 5 h after treatment.

subsequently be oxidized to carboxylic acids to terminate with the mineralization of the contaminants as depicted on the mechanism of Fig. 10. The corresponding numbers for each peak in the chromatogram are indicated in Table 5. Other double-ringed chemical species type biphenyls or phenoxy group as substituent were also identified, which generation become possible due to the composition of the aqueous solution. Some of these species have been reported by other authors when using advanced oxidation methods and UV radiation [56]. Moreover, low molecular weight carboxylic acids were also detected in the aqueous phase, but their separation by GC–MS is more complex due to their high polarity and solubility in water.

In Figs. 9(a) and (b), it is observed that the effect of the composition of the gas mixture on the generation of the by-products of the organic mixture oxidation, as seen in the figure the abundance of certain molecules decreased (retention time interval around 7–10 min) when the proportion of O_2 in gas mixture was increased around the same power supplied. It is also observed that some species were not detected when only O_2 gas was applied in comparison when Ar/ O_2 gas mixtures were used, indicating that they were not generated or promptly oxidized to smaller species as shown in Fig. 10 mechanism. 5 h later the treated samples were analyzed (Figs. 9(c) and (d)), which showed that the by-products were practically removed, as can be seen when only O_2 was

supplied. Also, gas samples were continuously collected at the gas outlet (Fig. 1) where CO_2 was detected qualitatively by GC/MS. Moreover, considering the acidity of the sample (low pH), degradation after plasma treatment was attributed to residual ozone in the aqueous solution. For the cases with a high content of Ar in the gas mixture, intermediates 1, 2, 4 and 6, see Table 5, were very recalcitrant by-product to oxidation by H_2O_2 residual. Other studies [23] have shown that even until 24 h after treatment, residual ozone can stay dissolved in aqueous solution contributing to the degradation of remaining low molecular weight organic compounds.

4. Conclusions

The thin-falling-water-film reactor using non-thermal plasma was successfully able to oxidize and remove the mixture of organic pollutants such as phenol and *m*-cresol in a same aqueous solution. It can be considered that the four types of gas mixture used in this study were highly efficient for the simultaneous removal of both organic compounds; highlighting that when supplying only O_2 the best elimination efficiencies of up to 99.2% for phenol and 99.6% for *m*-cresol were achieved. Also, when only O_2 was supplied a minor formation of intermediates was detected. In the first minutes of treatment, initially phenol was started to be degraded, generating by-products of its oxidation, all of them

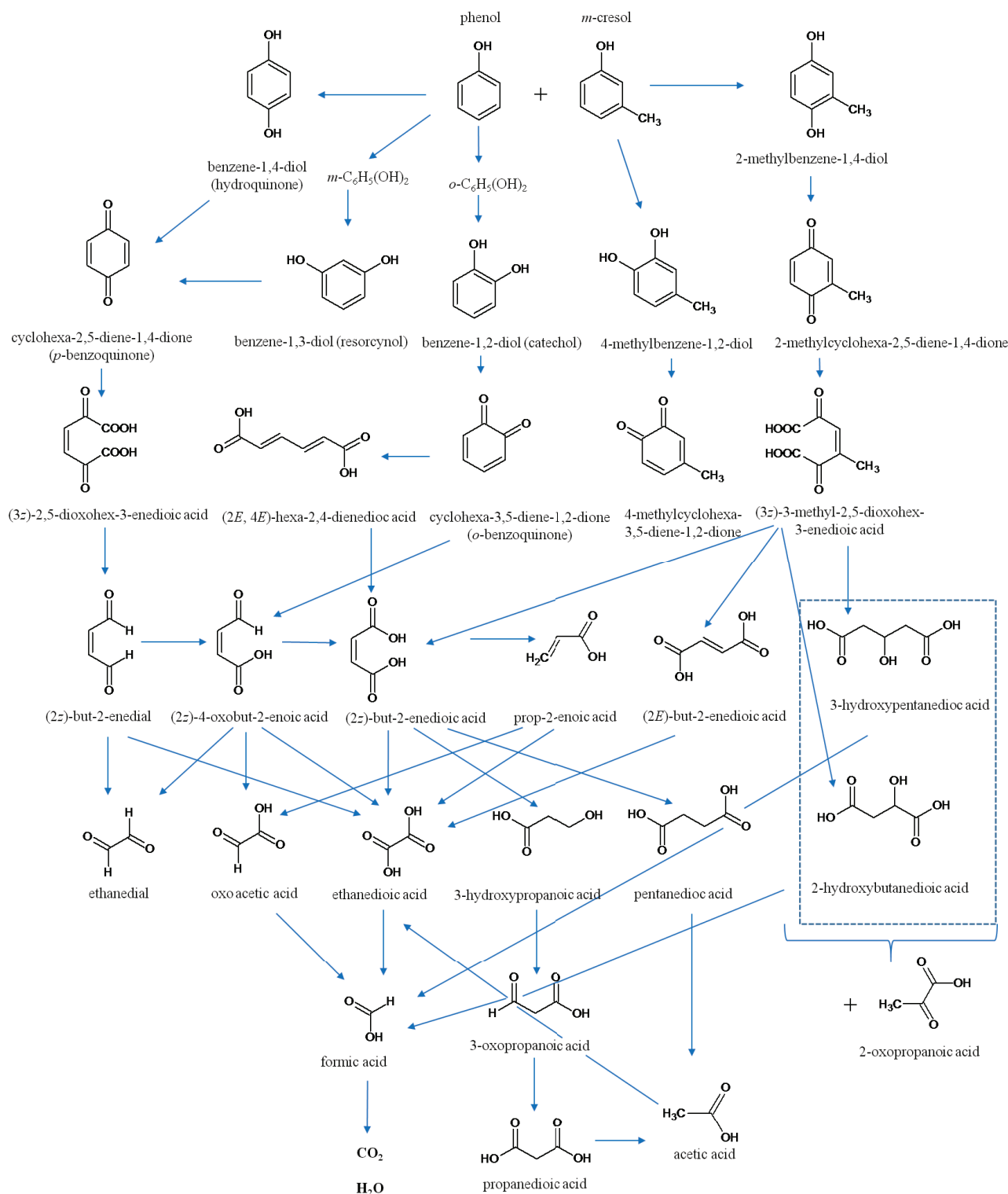
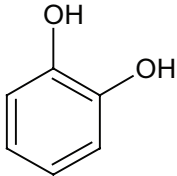
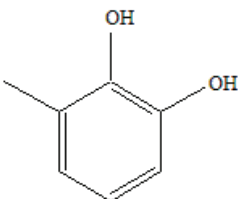
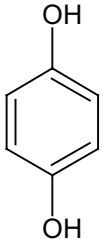
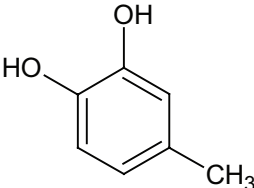
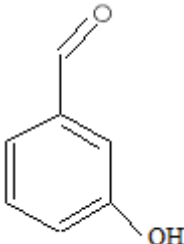
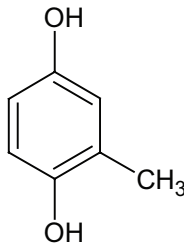
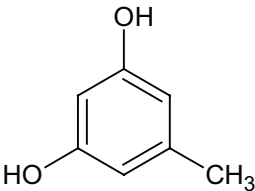
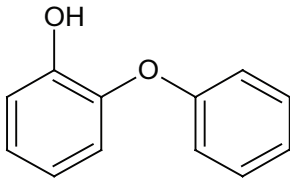
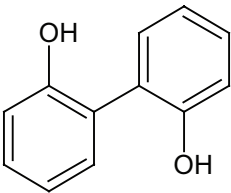
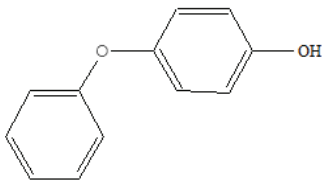
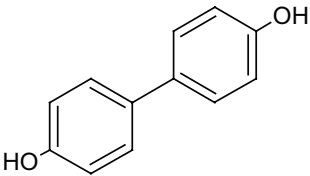


Fig. 10. Mechanism of oxidation of phenol and *m*-cresol.

have a lower acid dissociation constant (pK_a) than *m*-cresol hence they are oxidized faster. In addition to the difference in the reactivity of *ortho*-, *meta*- and *para*-substituents generated in relation to the groups $-OH$ (on phenol) and $-CH_3$ (on *m*-cresol), which promote the oxidation of phenol and its

by-products instead *m*-cresol. After 1 h of treatment, it was obtained a greater efficiency of degradation of *m*-cresol than that of phenol; this could be attributed to the concentration difference effect of phenol and *m*-cresol, which in certain time, when their magnitudes are comparables, the *m*-cresol

Table 5
Oxidation by-products of phenol and *m*-cresol organic mixture

No	Compound	Structure	No	Compound	Structure
1	Benzene-1,2-diol (catechol)		2	3-Methylbenzene-1,2-diol	
3	Benzene-1,4-diol (hydroquinone)		4	4-Methylbenzene-1,2-diol	
5	3-Hydroxybenzaldehyde		6	2-Methylbenzene-1,4-diol	
7	5-Methylbenzene-1,3-diol		8	2-Phenoxyphenol	
9	Biphenyl-2,2'-diol		10	4-Phenoxyphenol	
11	Biphenyl-4,4'-diol				

oxidation is more efficient than phenol oxidation. The experimental results were qualitatively validated from the simulating outcomes from the proposed simplified chemical kinetics model. This model fully allowed to validate in a descriptive way that phenol oxidation begins earlier than that of *m*-cresol,

nevertheless, after a certain period of time is evident that *m*-cresol oxidation becomes more efficient than phenol oxidation, this can be attributed to concentration effect and slightly larger reaction rate coefficient with regard to phenol, which is in agreement with the realized experimentation.

Acknowledgments

This work received financial support from CONACYT, Mexico. The authors appreciate the technical assistance received from M.T. Torres Martinez, P. Angeles Espinosa and I. Contreras Villa.

Symbols

A_0	—	Initial abundance of the contaminant
A_t	—	Abundance of the contaminant obtained at time t
C_o	—	Initial concentration of the contaminant
E	—	Supplied energy to DBD reactor
f	—	Frequency of the supplied AC voltage waveform
G	—	Amount of matter removed per unit of supplied input energy
i	—	Chemical species
k	—	Reaction rate coefficient
n_i	—	The density of “ i ” species
pK_a	—	Acid dissociation constant
S_i	—	The mass balance of “ i ” species
t	—	Time
tm	—	Time required to get 50% of contaminant removal
Vol	—	Volume of the aqueous solution
x	—	A constant representing 50% of contaminant removal
η	—	Degradation efficiency
σ_m	—	Hammett <i>meta</i> -substituent constant
σ_p	—	Hammett <i>para</i> -substituent constant
\varnothing_{ext}	—	External diameter

Superscript

* i — Denotes a radical of the “ i ” species

References

- [1] T. Olmez-Hanci, I. Arslan-Alaton, Comparison of sulfate and hydroxyl radical based advanced oxidation of phenol, *Chem. Eng. J.*, 224 (2013) 10–16.
- [2] L.G. Cordova Villegas, N. Mashhadi, M. Chen, D. Mukherjee, K.E. Taylor, N. Biswas, A short review of techniques for phenol removal from wastewater, *Curr. Pollut. Rep.*, 2 (2016) 157–167.
- [3] L.A. Cesar Teixeira, N. de A. Vieira Junior, L. Yokoyama, F. Valéria da Fonseca, Degradation of phenol in mine waters using hydrogen peroxide and commercial steel wool, *Int. J. Miner. Process.*, 138 (2015) 15–19.
- [4] M.M. Emara, N.H. Amin, S.M.K.A. Fotouh, M.M. El-Moselhy, M.S. Abd-El-Maqsoud, Kinetic studies of homogeneous photocatalytic degradation of phenol using H_2O_2 under different experimental conditions, *Int. J. Environ.*, 4 (2015) 322–335.
- [5] A.P.B. Rodriguez de Freitas, L. Valim de Freitas, H.J. Izário Filho, M. Borges Silva, Phenol removal via advanced oxidative processes (O_3 /photo-Fenton) and chemometrics, *Am. J. Theor. Appl. Stat.*, 2 (2013) 243–247.
- [6] Z. Zeng, H. Zou, X. Li, M. Arowo, B. Sun, J. Chen, G. Chu, L. Shao, Degradation of phenol by ozone in the presence of Fenton reagent in a rotating packed bed, *Chem. Eng. J.*, 229 (2013) 404–411.
- [7] M. Sayed, Efficient removal of phenol from aqueous solution by the pulsed high-voltage discharge process in the presence of H_2O_2 , *Chem. Int.*, 1 (2015) 81–86.
- [8] F. Ge, L. Zhu, H. Chen, Effects of pH on the chlorination process of phenols in drinking water, *J. Hazard. Mater.*, 133 (2006) 99–105.
- [9] F.J. Beltran, J.M. Encinar, J.F. Garcia-Araya, Ozonation of *o*-cresol in aqueous solutions, *Water. Res.*, 24 (1990) 1309–1316.
- [10] Y. Sun Mok, J.-O. Jo, Degradation of a textile azo dye by pulsed arc discharge to the surface of wastewater, *Korean J. Chem. Eng.*, 24 (2007) 607–611.
- [11] W. Wang, S. Wang, J. Feng, S. Yuan, Z. Hu, J. Muñoz Sierra, X. Zhang, Kinetics of hydroquinone oxidation by a wire-cylinder dielectric barrier discharge reactor, *Desal. Wat. Treat.*, 57 (2016) 29212–29219.
- [12] D. Gumuchian, S. Cavadias, X. Duten, M. Tatoulian, P. Da Costa, S. Ognier, Organic pollutants oxidation by needle/plate plasma discharge: on the influence of the gas nature, *Chem. Eng. Process. Process Intensif.*, 82 (2014) 185–192.
- [13] S. Esplugas, J. Giménez, S. Contreras, E. Pascual, M. Rodríguez, Comparison of different advanced oxidation processes for phenol degradation, *Water Res.*, 36 (2002) 1034–1042.
- [14] M. Choquette-Labbé, W.A. Shewa, J.A. Lalman, S.R. Shanmugam, Photocatalytic degradation of phenol and phenol derivatives using a nano-TiO₂ catalyst: integration quantitative and qualitative factors using response surface methodology, *Water*, 6 (2014) 1785–1806.
- [15] G. Wang, D. Xu, W. Guo, X. Wei, Z. Sheng, Z. Li, Preparation of TiO₂ nanoparticle and photocatalytic properties on the degradation of phenol, *Conf. Ser. Earth Environ. Sci.*, 59 (2017) 012046.
- [16] B. Jiang, J. Zheng, S. Qiu, M. Wu, Q. Zhang, Z. Yang, Q. Xue, Review on electrical discharge plasma technology for wastewater remediation, *Chem. Eng. J.*, 236 (2014) 348–368.
- [17] M. Hijosa-Valsero, R. Molina, H. Schikora, M. Müller, J.M. Bayona, Removal of priority pollutants from water by means of dielectric barrier discharge atmospheric plasma, *J. Hazard. Mater.*, 262 (2013) 664–673.
- [18] J. Feng, L. Jiang, D. Zhu, K. Su, D. Zhao, J. Zhang, Z. Zheng, Dielectric barrier discharge plasma induced degradation of aqueous atrazine, *Environ. Sci. Pollut. Res. Int.*, 23 (2016) 9204–9214.
- [19] C. Sarangapani, N.N. Misra, V. Milosavljevic, P. Bourke, F. O’Regan, P.J. Cullen, Pesticide degradation in water using atmospheric air cold plasma, *J. Water Proc. Eng.*, 9 (2016) 225–232.
- [20] C. Sarangapani, Y. Dixit, V. Milosavljevic, P. Bourke, C. Sullivan, P.J. Cullen, Optimization of atmospheric air plasma for degradation of organic dyes in wastewater, *Water Sci. Technol.*, 75 (2017) 207–219.
- [21] G. Son, H. Lee, J.-E. Gu, S. Lee, Decoloration of methylene blue hydrate by submerged plasma irradiation process, *Desal. Wat. Treat.*, 54 (2015) 1445–1451.
- [22] L. Xin, Y. Sun, J. Feng, J. Wang, D. He, Degradation of triclosan in aqueous solution by dielectric barrier discharge plasma combined with activated carbon fibers, *Chemosphere*, 144 (2016) 855–863.
- [23] D. Manojlović, D.R. Ostojic, B.M. Obradović, M.M. Kuraica, V.D. Krsmanović, J. Purić, Removal of phenol and chlorophenols from water by new ozone generator, *Desalination*, 213 (2007) 116–122.
- [24] B.P. Dojčinović, D. Manojlović, G.M. Roglić, B.M. Obradović, M.M. Kuraica, J. Purić, Plasma assisted degradation of phenol solutions, *Vacuum*, 83 (2009) 234–237.
- [25] H.H. Cheng, S.S. Chen, K. Yoshizuka, Y.C. Chen, Degradation of phenolic compounds in water by non-thermal plasma treatment, *J. Water Chem. Technol.*, 34 (2012) 179–189.
- [26] P. Lukes, B.R. Locke, Degradation of substituted phenols in hybrid gas-liquid electrical discharge reactor, *Ind. Eng. Chem. Res.*, 44 (2005) 2921–2930.
- [27] M.D. Gurol, S. Nekouinaini, Kinetic behavior of ozone in aqueous solutions of substituted phenol, *Ind. Eng. Chem. Fundam.*, 23 (1984) 54–60.
- [28] C. Kennes, J.M. Lema, Simultaneous biodegradation of *p*-cresol and phenol by the basidiomycete *Phanerochaete chrysosporium*, *J. Ind. Microbiol.*, 13 (1994) 311–314.
- [29] J. Araña, V.M. Rodríguez López, E. Pulido Melián, M.I. Suárez Reyes, J.M. Doña Rodríguez, O. González Díaz, Comparative study of phenolic compounds mixtures, *Catal. Today*, 129 (2007) 177–184.

- [30] B. Jaramillo-Sierra, A. Mercado-Cabrera, R. López-Callejas, J. A. López-Fernández, R. Peña-Eguiluz, S.R. Barocio, R. Valencia-Alvarado, B. Rodríguez-Méndez, A. Muñoz-Castro, A. de la Piedad-Beneitez, Phenol degradation in aqueous solution by a gas-liquid phase DBD reactor, *Eur. Phys. J. Appl. Phys.*, 56 (2011) 24026.
- [31] B. Jaramillo-Sierra, A. Mercado-Cabrera, R. López-Callejas, R. Peña-Eguiluz, S.R. Barocio, R. Valencia-Alvarado, B. Rodríguez-Méndez, A.E. Muñoz-Castro, A. de la Piedad Beneitez, Degradation of *m*-cresol in aqueous solution by dielectric barrier discharge, *J. Phys. Conf. Ser.*, 406 (2012) 012025.
- [32] A.A. Joshi, B.R. Locke, P. Arce, W.C. Finney, Formation of hydroxyl radicals, hydrogen peroxide and aqueous electrons by pulsed streamer corona discharge in aqueous solution, *J. Hazard. Mater.*, 41 (1995) 3–30.
- [33] D.R. Grymonpré, A.K. Sharma, A.W.C. Finney, B.R. Locke, The role of Fenton's reaction in aqueous phase pulsed streamer corona reactors, *Chem. Eng. J.*, 82 (2001) 189–207.
- [34] M. Dors, G.V. Nichipor, J. Mizeraczyk, Modeling of Phenol Decomposition Induced by Pulsed Corona Discharge in Water, *Proc. IEEE International Conference on Dielectric Liquids (ICDL 2005)*, Coimbra, Portugal, 26 June–1 July 2005.
- [35] V. Kavitha, K. Palanivelu, Destruction of cresols by Fenton oxidation process, *Water Res.*, 39 (2005) 3062–3072.
- [36] M. Dors, E. Metel, J. Mizeraczyk, Phenol degradation in water by pulsed streamer corona discharge and Fenton reaction, *Int. J. Plasma Environ. Sci. Technol.*, 1 (2007) 76–81.
- [37] M. Pimentel, Phenol and Cresols Treatment in Aqueous Solution by Electro-Fenton Process: Application to the Mineralization of Aeronautic Wastewater Industry, PhD Dissertation, Université Paris-Est Marne-La-Vallée, September 2008.
- [38] D.X. Liu, P. Bruggeman, F. Iza, M.Z. Rong, M.G. Kong, Global model of low-temperature atmospheric-pressure He+H₂O plasmas, *Plasma Sources Sci. Technol.*, 19 (2010) 025018.
- [39] M.R. Rojas, F. Pérez, D. Whitley, R.G. Arnol, A.E. Sáez, Modeling of advanced oxidation of trace organic contaminants by hydrogen peroxide photolysis and Fenton's reaction, *Ind. Eng. Chem. Res.*, 49 (2010) 11331–11343.
- [40] B.A. Gottwald, G. Warner, A reliable Rosenbrock integrator stiff differential equations, *Computing*, 26 (1981) 355–360.
- [41] W.H. Press, S.A. Teukolsky, W.T. Vetterling, B.P. Flannery, *Numerical Recipes in Fortran 77: The Art of Scientific Computing*, Chapter 16.6, Cambridge University Press 1986, 1992.
- [42] D. Gardoni, A. Vailati, R. Canziani, Decay of ozone in water: a review, *Ozone Sci. Eng.*, 34 (2012) 233–242.
- [43] M.C. Valsania, F. Fasano, S.D. Richardson, M. Vincenti, Investigation of the degradation of cresols in the treatments with ozone, *Water Res.*, 46 (2012) 2795–2804.
- [44] D.R. Lide, Editor-in-Chief, *CRC Handbook of Chemistry and Physics*, 90th ed., CRC Press (an imprint of Taylor and Francis), Boca Raton, FL, 2009.
- [45] C. Hansch, A. Leo, R.W. Taft, A survey of Hammett substituent constants and resonance and field parameters, *Chem. Rev.*, 91 (1991) 165–195.
- [46] M. Tezuka, M. Iwasaki, Plasma induced degradation of chlorophenols in an aqueous solution, *Thin Solid Films*, 316 (1998) 123–127.
- [47] P. Neta, R.E. Huie, A.B. Ross, Rate constants for reactions of inorganic radicals in aqueous solution, *J. Phys. Chem. Ref. Data*, 17 (1988) 1027–1284.
- [48] S. Khuntia, S.K. Majumber, P. Ghosh, Quantitative prediction of generation of hydroxyl radicals from ozone microbubbles, *Chem. Eng. Res. Des.*, 98 (2015) 231–239.
- [49] A.A. Garamoon, F.F. Elakshar, A.M. Nossair, E.F. Kotp, Experimental study of ozone synthesis, *Plasma Sources Sci. Technol.*, 11 (2002) 254–259.
- [50] W.F.L.M. Hoeben, E.M. van Veldhuizen, W.R. Rutgers, C.A.M.G. Cramers, G.M.W. Kroesen, The degradation of aqueous phenol solutions by pulsed positive corona discharges, *Plasma Sources Sci. Technol.*, 9 (2000) 361–369.
- [51] D.R. Grymonpré, W.C. Finney, R.J. Clark, B.R. Locke, Hybrid gas-liquid electrical discharge reactors for organic compound degradation, *Ind. Eng. Chem. Res.*, 43 (2004) 1975–1989.
- [52] H. Kušić, N. Koprivanac, B.R. Locke, Decomposition of phenol by hybrid gas/liquid electrical discharge reactors with zeolite catalysts, *J. Hazard. Mater.*, 125 (2005) 190–200.
- [53] E. Marotta, E. Ceriania, M. Schiorlina, C. Cerettab, C. Paradisia, Comparison of the rates of phenol advanced oxidation in deionized and tap water within a dielectric barrier discharge reactor, *Water Res.*, 46 (2012) 6239–6246.
- [54] G.V. Buxton, C.L. Greenstock, W.P. Helman, A.B. Ross, Critical review of rate constants for reactions of hydrated electrons, hydrogen atoms and hydroxyl radicals ([•]OH/[•]O) in aqueous solution, *J. Phys. Chem. Ref. Data*, 17 (1988) 513–886.
- [55] Y. Zheng, D.O. Hill, C.H. Kuo, Destruction of cresols by chemical oxidation, *J. Hazard. Mater.*, 34 (1993) 245–260.
- [56] M. Farzadkia, Y.D. Shahamat, S. Nasser, A.H. Mahvi, M. Gholami, A. Shahryari, Catalytic ozonation of phenolic wastewater: identification and toxicity of intermediates, *J. Eng.*, 2014 (2014) 1–10.